tag: sPH-HF-2023-003
version: 0.1
DOI: unspecified
date: August 15, 2023

D-meson tagged jets in sPHENIX

Antonio Silva
Iowa State University
Xuan Li
Los Alamos National Laboratory

Abstract

The sPHENIX experiment will perform the first bottom hadron and jet measurements to study the properties of the created Quatk Gluon Plasma (QGP) in heavy ion collisions. Charm-hadron inside jet production in $p + p$ and A+A collisions can not only help revealing the flavor-dependent energy loss in different nuclear medium conditions, but also provide the direct insight on the charm quark hadronization process. The KFParticle and ParticleFlow algorithms have been implemented in the sPHENIX software framework for heavy flavor jet reconstructions. Jets tagged with the presence of a D-meson as one of their constituents are selected as jets originating from heavy-flavor quark fragmentation. In this note, we report the first D^0-jet studies in $p + p$ simulation. The tagging algorithm discussed in this note will be optimized for Au+Au collisions and ongoing Au+Au simulation studies will be reported in another note.

1 Introduction

Heavy flavor jet production at RHIC has its unique features compared to LHC measurements. Lower jet transverse momentum coverage can be accessed by the sPHENIX measurements than existing LHC results. Moreover, less recombination effects are expected for the sPHENIX heavy flavor measurements compared to LHC studies [1], which will result in a different nuclear modification of sPHENIX heavy flavor production [2]. This notes summarizes the latest simulation studies for D^0 tagged jets in 200 GeV $p+p$ collisions, which have different fragmentation functions from bottom jets (b-jets).

Jets tagged with the presence of a D-meson as one of their constituents are selected as jets originating from heavy-flavor quark fragmentation. This note presents the 2D η versus ϕ raw distributions of D^0-jets and 2D D^0-jet versus D^0 raw transversal momentum distribution. None of the figures have been corrected by D^0-jet reconstruction efficiency or detector effects (unfolding), which will be evaluated later.

2 Simulation

The figures presented in this note are from PYTHIA8 [3] simulations of p+p collisions at $\sqrt{s}$ = 200 GeV without pileup and tuned to the minimum bias condition environment at RHIC [4]. The generated events were required to have at least one $c\bar{c}$ in order to enhance the production of D^0 mesons and at least one jet with a minimum transverse momentum of 5 GeV/c or 12 GeV/c in order to enhance the jet sample. The PYTHIA 8 configuration is listed below:

- PDF:pSet = 13
- HardQCD:hardccbar = on
- SoftQCD:inelastic = off
- Charmonium:all = off
- D-mesons (411,421,413,...) onMode = off
- 421:onIfMatch = 321 -211
- 421:onIfMatch = -321 211
- ColourReconnection:mode = 2
- TimeShower:alphaSvalue = 0.18
- PhaseSpace:pTHatMin = 5.0 (production tag 17) or 12 (production tag 18).

Here NNPDF2.3 QCD+QED LO PDF set is used, NLO $\alpha_s(M_Z)$ equals to 0.130.

The sPHENIX detector was simulated using GEANT4[5] and the events were fully reconstructed taking into account all subsystems in the central barrel, but also the beam pipe and detectors are forward and backward rapidity like the Minium Bias Detector (MBD) and the Event Plane Detector (sEPD).

In the central barrel, the closest detector to the beam pipe if the monolithic active pixel sensor vertex detector (MVTX). Going away from the beam pipe, the next detector after the MVTX is the Intermediate Tracker (INTT). These two detectors are the vertex detectors responsible for providing the reconstruction of the D-meson decay topology. The INTT will also provide fast timing for rejecting most of the pile-up expected to be seen in p+p collisions.

Continuing outwards, the next detector is the Time-Projection Chamber, which is the main tracking detector responsible for precise track momentum reconstruction, which is a key element for good D^0 transverse momentum resolution.

After the tracking detectors is where the Electromagnetic Calorimeter (EMCal) is located, followed by the Inner Hadronic Calorimeter (IHCal), a magnet operating in 1.4 T and, finally, the Outer Hadronic Calorimeter (OHCal). The information from the calorimeters is combined with tracks in a sPHENIX implementation of particle flow. Charged particles in particle flow are dominated by tracks, which have a p_T resolution better than 2% for particles in the range $0.5 < p_{T,track} < 10$ GeV/c [6]. Particles that do not leave a track in the tracking detectors are reconstruct by the calorimeters and their resolution depend on the specific subsystem [7]. Photon reconstruction is mainly driven by the EMCal, which count on energy resolution of $3\% \bigoplus 16\%/\sqrt{E}$. Neutral hadrons, such as K^0, are reconstructed by the HCAL, with a resolution of $14\% \bigoplus 65\%/\sqrt{E}$. The energy resolution that depend on particle species affects the reconstructed energy of the jet tagged by D-mesons, which has to be corrected by unfolding [8].

3 Software and reconstruction method

The first step in the D-jet reconstruction is the reconstruction of D mesons candidates. This is done using KFParticle [9] developed by the CBM Collaboration and adapted to Fun4All in sPHENIX. The code has been updated with small bug fixes but remains basicaly the same used and presented in previous works [10].

Particle flow elements are reconstructed with the combination of tracks and topo-clusters. The method used for topo-cluster reconstruction in sPHENIX is very similar to the one used by ATLAS Collaboration [11]. In sPHENIX, two different types of topo-clusters are reconstructed:

- EMCal topo-clusters: reconstructed using only the information of the EMCal
- HCal topo-clusters: 3D topological clusters reconstructed using the IHCal and OHCal

The 3D topological clusters will cluster towers not only close in η and ϕ but also considers towers in the two layers of the HCal. The clusterization procedure mainly depends on a seed parameter (S) and a growth parameter (N). The S parameter is an integer number that dictates the minimum required energy for a tower to be selected as a seed that will start a clusterization process. The minimum energy is defined as a product of the S parameter and the noise of the given detector. The noise in the calorimeters was studied during the beam test of the calorimeters [12] and, the current values used are 0.03 GeV for the EMCal, 0.0025 GeV for the IHCal and 0.006 GeV for the OHCal. Currently, for p+p collisions, the values used are $S = 4$ and $N = 2$;

Once the seeds are identified based on the S parameter criterion, they are ordered in descending order for the clusterization process. The minimum required energy for a tower in the neighborhood of a seed to be merged is given by the g parameter, which is multiplied by the average noise of the detector in the same way done for the seed criterion. For the HCal topo-clusters, the towers in the upper (if the seed is located in the IHCal) or lower layer (if the seed is located in the OHCal) are also considered as neighbor towers.

The topo-clusters are then combined with tracks in such a way to avoid double counting of signals. Initially the tracks are projected outward up to the EMCal and OHCal radii establishing the η and ϕ positions of the track in the given calorimeter. All topo-clusters satisfying a $\Delta R = \sqrt{(\eta_{track} - \eta_{cluster})^2 + (\phi_{track} - \phi_{cluster})^2} < 0.2$ are associated with the track.

The way particles are solved follows the CMS approach [13] in a very similar way. At the end, clusters associated with a track and considered to be the same particle are removed and the track kinematics is used to create a particle flow element considering the mass of a charged pion. Topo-clusters not associated with tracks are used and identified as photons (EMCal topo-clusters) or neutral hadrons (HCal topo-clusters).

The code for topo-cluster and particle flow reconstruction can be found in the sPHENIX coresoftware repository (https://github.com/sPHENIX-Collaboration/coresoftware/blob/master), respectively in /offline/packages/CaloReco/RawClusterBuilderTopo.cc and /offline/packages/particleflow/ParticleFlowReco.cc.

The D-jet reconstruction module is also in the sPHENIX coresoftware and can be found in the directory /offline/packages/ResonanceJetTagging. This module is capable of reconstruct jets tagged with any D-meson species reconstructed by KFParticle and particle flow elements using the FastJet [14] software. The reconstruction strategy consists in removing from the event the particle flow elements associated to the D-meson decay daughters and replace them by the D-meson 4-momentum vector. This scheme is pictured in figure 1 and makes the determination of which jet contains the D-meson univocal. In the past, jets were tagged by using the geometrical distance in the η and ϕ phase space of the D-meson and the jet [15], which should be smaller than the jet resolution parameter R. This could create cases where none (or only part) of the D meson decay daughters were in fact constituents of the jet, originating problems when calculating observables such as the D-jet momentum fraction.

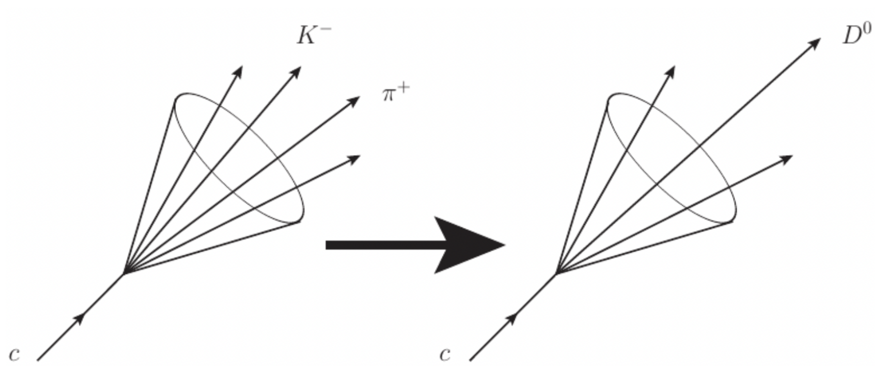

Figure 1: D^0-jet reconstruction scheme. D^0 decay daughters are replaced by the D^0 4-momentum vector

Another issue the code addresses is the possibility of having two D-meson candidates sharing the same decay daughter. This is pictured in figure 2 where two D^0 candidates where identified with different charged pions but sharing the same kaon. This is maybe unlikely in low multiplicity events like p+p collisions depending on the selections applied to the decay daughters, but becomes more common in heavy-ion collisions and has to be taken into account. The strategy to solve this issue is to remove the particle flow elements associated with the D-meson decay daughter and replace them by the D-meson 4-momentum vector for every D-meson candidate. This selection aims to remove any p_T selection biases. This means that jets will be reconstructed once per D-meson candidate and will create one D-jet candidate for each D-meson candidate.

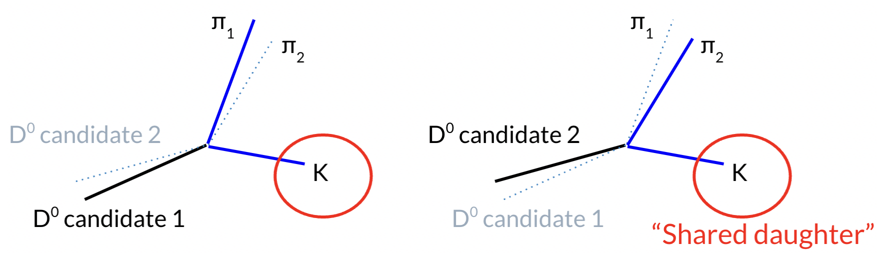

Figure 2: Illustration of the daughter sharing problem. D^0 candidate 1 is reconstructed from π_1 and the kaon and candidate 2 from π_2 and the same kaon.

In simulations, the match between the D^0-jets from fully reconstructed signals and D^0-jets from generated level particles from PYTHIA8 is done by the presence of the same D^0 in generated and reconstructed levels. Again, no geometric criterion is necessary.

4 Cut selection

All figures presented in this note use the anti-k_t algorithm. The jet resolution parameter (cone radius), R, is selected at 0.4, and the E-scheme is used for the jet reconstruction.

The D^0 selection cuts, which use the same cut selection in sPH-HF-2023-01 [16], are listed below:

- Track $p_T > 0.7$ GeV/c;
- Track χ^2/NDF < 5;
- Track IP > 0.0025 cm;
- Track IP $\chi^2 < 3$;
- Track-Track DCA < 0.008 cm;
- Recon D^0 χ^2/NDF < 5;
- Recon D^0 DIRA > 0.9;
- Recon D^0 mass in [1.7,2.0] GeV/c^2;
- Recon D^0 $p_T > 1.5$ GeV/c (3.0 GeV/c).

The alternative D^0 $p_T > 3.0$ GeV/c was chosen to study the same kinematic distributions with less combinatorial backgrounds and better DCA resolution. Plots with this cut are documented in another note.

The D^0-jet selection cuts are listed below:

- Require the jet to contain a D^0 and at least another particle;
- Jet $p_T > 7$ GeV/c (10 GeV/c);
- Reconstructed Jet mass > reconstructed D^0 mass + 0.5 GeV/c^2;
- Uses the default calorimeter noise setting and energy threshold cuts in the sPHENIX Particle-Flow algorithm.

The alternative jet $p_T > 10.0$ GeV/c was applied together with the D^0 $p_T > 3.0$ GeV/c cut. Plots with this cut are documented in another note.

Two sPHENIX D^0-jet simulation samples have been produced, one sample contains 1M events with the 5 GeV/c $\hat{p}_{T,min}$ selection and the other sample contains 1M events with the 12 GeV/c $\hat{p}_{T,min}$ selection. This note only contains the D^0 tagged jet related kinematics using the sPHENIX D^0-jet simulation with the 12 GeV/c $\hat{p}_{T,min}$ selection. Other distributions using both the 5 GeV/c and 12 GeV/c simulations will be documented in a separate note.

5 Results of the reconstructed D^0 kinematics

The kinematics of the D^0 and D^0-jet at the truth and reconstruction levels have been extensively studied. Here we only present selected kinematic distributions. It's important to first validate the D^0's kinematics in simulation as these D^0s are the seeds to form D^0 tagged jets.

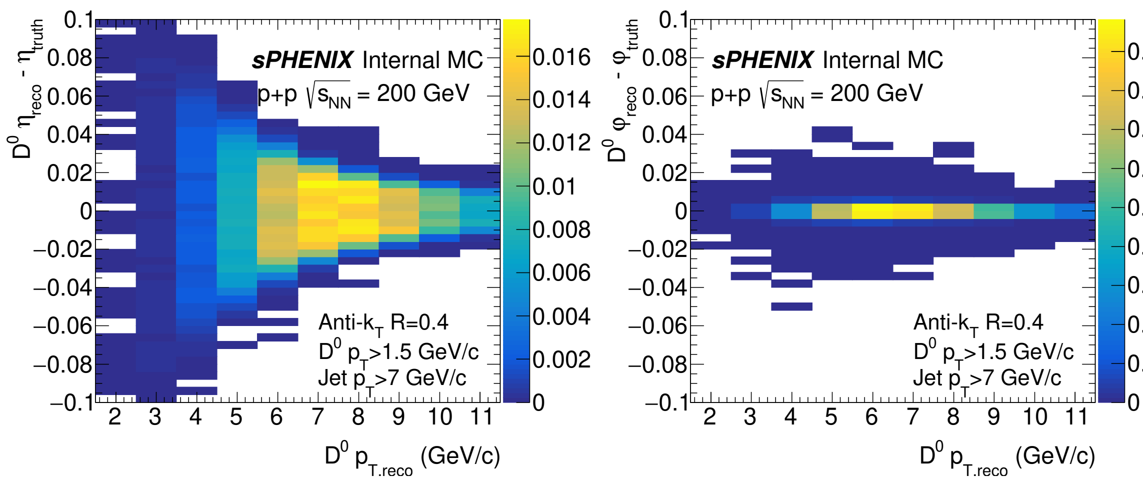

Figure 3: The reconstructed D^0 p_T dependent η_{reco}-η_{truth} (left) and reconstructed D^0 p_T dependent φ_{reco}-φ_{truth} (right) using the sPHENIX 12 GeV D^0-jet simulation samples. Jets are reconstructed with the Anti-k_T algorithm and the cone radius is at 0.4. The selection cuts include D^0 $p_T > 1.5$ GeV/c and the D^0 tagged jet $p_T > 7$ GeV/c.

Figure 3 shows the reconstructed D^0 p_T dependent η_{reco}-η_{truth} (left) and reconstructed D^0 p_T dependent φ_{reco}-φ_{truth} distributions using the sPHENIX 12 GeV D^0-jet simulation samples. These D^0s are required to be within the jet cone (R=0.4) and reconstructed D^0 $p_T > 1.5$ GeV/c. Both distributions of Figure 3 are normalized by the total counts of selected D^0-jets. Meanwhile the D^0 tagged jet p_T is greater than 7 GeV/c. Reconstructed D^0 pseudorapidity has a strong dependence on the reconstructed D^0 p_T. For high p_T D^0s, the psedorapidity resolution is better than 0.05 and the azimuthal angle resolution is better than 0.04.

6 Results of the D^0-jet kinematics

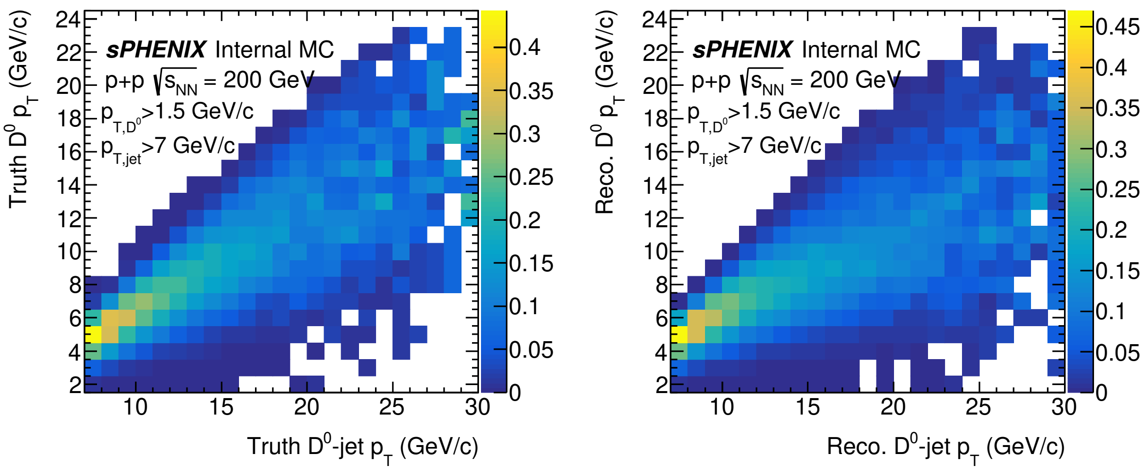

Figure 4: $p_{T,truth}$ of D^0 versus $p_{T,truth}$ of D^0 tagged jets (left). $p_{T,reco}$ of D^0 versus $p_{T,reco}$ of D^0 tagged jets (right). These distributions are obtained with the sPHENIX 12 GeV D^0-jet simulation samples. Jets are reconstructed with the Anti-k_T algorithm and the cone radius is at 0.4. The selection cuts include D^0 $p_T > 1.5$ GeV/c and the D^0 tagged jet $p_T > 7$ GeV/c.

The kinematics of the D^0 tagged jet have been studied as well. Figure 4 shows the 2D correlation plot of D^0 p_T versus D^0 tagged jet p_T at the truth level (left) and the reconstruction level (right). These distributions use the sPHENIX 12 GeV D^0-jet simulation samples. The distributions in Figure 4 are normalized per y axis slice. This normalization method aims to mitigate the p_T dependence biases. Similar correlation patterns have been observed in the D^0 p_T versus D^0 tagged jet p_T at the truth and reconstruction levels, which indicates that the D^0 jet tagging algorithm works as expected. Further detailed studies to understand the D^0 tagged jet jet energy scale (JES), jet energy resolution (JER), tagging efficiency and purity are underway. We plan to implement the same jet algorithm for Run2024 $p+p$ data and apply further optimizations in the data analysis.

References

[1] ALICE Collaboration. First measurement of λ_c baryon production in au+au collisions at $\sqrt{s} = 200$ gev. *Physical Review Letters*, 124(17), may 2020. 1

[2] sPHENIX Collaboration. 2022 sPHENIX Beam Use Proposal. URL: `https://indico.bnl.gov/event/15845/attachments/40963/68517/sPHENIX_Beam_Use_Proposal_2022.pdf`. 1

[3] Torbjörn Sjöstrand, Stephen Mrenna, and Peter Skands. A brief introduction to PYTHIA 8.1. *Computer Physics Communications*, 178(11):852–867, 2008. 2

[4] W Park S. Lim. Pythia8 tune in pp 200 gev. *Presentation at Heavy FlavorTopical Group Meeting*, Dec 2020. URL: https://indico.bnl.gov/event/10309/contributions/44139/attachments/31909/50542/sPHENIX_HF_shlim_20201215.pdf. 2

[5] S. Agostinelli et al. Geant4—a simulation toolkit. *Nuclear Instruments and Methodsin Physics Research Section A: Accelerators, Spectrometers, Detectors and AssociatedEquipment*, 506(3):250–303, 2003. 2

[6] Joseph D. Osborn, Anthony D. Frawley, Jin Huang, Sookhyun Lee, Hugo Pereira Da Costa, Michael Peters, Christopher Pinkenburg, Christof Roland, and Haiwang Yu. Implementation of ACTS into sPHENIX track reconstruction. *Computing and Software for Big Science*, 5(1), oct 2021. 2

[7] C. A. Aidala et al. Design and beam test results for the sPHENIX electromagnetic and hadronic calorimeter prototypes. *IEEE Transactions on Nuclear Science*, 65(12):2901–2919, dec 2018. 2

[8] G. D'Agostini. A multidimensional unfolding method based on bayes' theorem. *Nuclear Instruments and Methods in Physics Research Section A: Accelerators, Spectrometers, Detectors and Associated Equipment*, 362(2):487–498, 1995. 2

[9] A. Gorbunov and I. Kisel. Reconstruction of decayed particles based on the Kalmanfilter. 2007. arXiv:CBM-SOFT-note-2007-003. 3

[10] J. Huang H. Okawa S. T. Araya, C. Dean and Z. Shi. First MDC1 Results fromHeavy Flavor Topical Group. 2021. 3

[11] ATLAS Collaboration. Topological cell clustering in the ATLAS calorimeters and its performance in LHC run 1. *The European Physical Journal C*, 77(7), 2017. 3

[12] C. A. Aidala et al. Design and beam test results for the sPHENIX electromagnetic and hadronic calorimeter prototypes. *IEEE Transactions on Nuclear Science*, 65(12):2901–2919, 2018. 3

[13] CMS Collaboration. Particle-flow reconstruction and global event description with the CMS detector. *Journal of Instrumentation*, 12(10):P10003–P10003, 2017. 3

[14] G. P. Salam M. Cacciari and G. Soyez. Topological cell clustering in the ATLAS calorimeters and its performance in LHC run 1. *The European Physical Journal C*, 1896, 2012. 3

[15] B. I. et al. Abelev. Measurement of D^* mesons in jets from $p+p$ collisions at $\sqrt{s} = 200$ GeV. *Phys. Rev. D*, 79:112006, Jun 2009. 3

[16] Cameron Dean. $D^0 \to K\pi^+$ modelling and selection in min-bias Au+Au simulations at sPHENIX=. URL: https://indico.bnl.gov/event/20254/attachments/49036/83522/D0_in_AuAu_MDC2_v1.0.pdf. 4